

İSTANBUL TECHNICAL UNIVERSITY ★ INSTITUTE OF SCIENCE AND TECHNOLOGY

**LEPTON-PAIR PRODUCTION IN RELATIVISTIC HEAVY ION COLLISIONS :
COULOMB CORRECTIONS TO TWO PHOTON MONTE CARLO MODEL**

**M.Sc. Thesis by
Fatma Pınar ASLAN**

Department : Physics Engineering

Programme : Physics Engineering

JUNE 2009

**LEPTON-PAIR PRODUCTION IN RELATIVISTIC HEAVY ION COLLISIONS :
COULOMB CORRECTIONS TO TWO PHOTON MONTE CARLO MODEL**

**M.Sc. Thesis by
Fatma Pınar ASLAN
(509061106)**

Date of submission : 4 May 2009

Date of defence examination : 3 June 2009

Supervisor (Chairman) : Prof. Dr. M. Cem GÜÇLÜ (ITU)
Members of the Examining Committee : Prof. Dr. Nafiye Güneç KIYAK (IU)
Prof. Dr. Ömer Faruk DAYI (ITU)

JUNE 2009

**RÖLATİVİSTİK HIZLARDAKİ AĞIR İYON ÇARPIŞMALARINDA
LEPTON ÇİFTİ ÜRETİMİ:
İKİ FOTON MONTE CARLO YÖNTEMİNE COULOMB DÜZELTMELERİ**

**YÜKSEK LİSANS TEZİ
Fatma Pınar ASLAN
(509061106)**

Tezin Enstitüye Verildiği Tarih : 4 Mayıs 2009

Tezin Savunulduğu Tarih : 3 Haziran 2009

**Tez Danışmanı : Prof. Dr. M. Cem GÜÇLÜ (İTÜ)
Diğer Jüri Üyeleri : Prof. Dr. Nafiye Güneç KIYAK (İÜ)
Prof. Dr. Ömer Faruk DAYI (İTÜ)**

HAZİRAN 2009

FOREWORD

I would like thank my supervisor Prof. Dr. Cem GÜÇLÜ for supporting me throughout my studies and for his encouragements.

I thank Prof. Dr. Nafiye G. KIYAK for helping me to make my dreams come true.

I also want to thank my dear friend Pamir TALAZAN for being there whenever i needed.

May 2009

Fatma Pınar ASLAN

Physics Engineer

TABLE OF CONTENTS

	<u>Page</u>
ABBREVIATIONS	ix
LIST OF TABLES	xi
LIST OF FIGURES	xiii
LIST OF SYMBOLES	xv
SUMMARY	xvii
ÖZET	xix
1. INTRODUCTION	1
2. SEMICLASSICAL APPROACH	3
3. TWO PHOTON APPROACH	7
4. MONTE CARLO SOLUTION	9
5. MULTI-PAIR PRODUCTION	11
6. COULOMB CORRECTIONS	13
7. CORRECTION IN Au-Au COLLISIONS	15
8. CORRECTION IN Pb-Pb COLLISIONS	21
9. CONCLUSION	27
REFERENCES	29
CIRRICULUM VITA	31

ABBREVIATIONS

QGP	:	Quark-gluon Plasma
RHIC	:	Relativistic Heavy Ion Collider
LHC	:	Large Hadron Collider
MC	:	Monte Carlo
Corr.	:	Corrected
int	:	Interaction

LIST OF TABLES

	<u>Page</u>
Table 7.1 : Total pair cross sections for Au-Au collisions.	17
Table 7.2 : Total pair cross sections for Au-Au collisions with $a = 1.8\lambda_c$. .	18
Table 8.1 : Total pair cross sections for Pb-Pb collisions.	23
Table 8.2 : Total pair cross sections for Pb-Pb collisions with $a = 4.7\lambda_c$. .	24

LIST OF FIGURES

	<u>Page</u>
Figure 2.1 : Schematic diagram of a relativistic heavy ion collision	3
Figure 2.2 : Coordinate frames	4
Figure 3.1 : The direct(a) and indirect(b) Feynmann diagrams for pair production in a heavy ion-collision	7
Figure 4.1 : The function of $F(q)$ verses q for the charges of the heavy-ions between $Z_{1,2} = 20 - 90$ and for the energies between $\gamma = 10 - 3400$.	10
Figure 5.1 : An example of a diagram included.	12
Figure 5.2 : Diagrams which are not included.	12
Figure 6.1 : The interaction between the produced pairs and the fields of heavy ions.	13
Figure 7.1 : Probability of producing N-pairs in a Au-Au as a function of impact parameter b with $\gamma = 100$ in two photon Monte Carlo model. Solid lines are the corrected calculations, and the dashed are the calculations without corrections	16
Figure 7.2 : Differential cross section for the N-pair production in Au-Au collision with $\gamma = 100$ in two photon Monte Carlo model. Solid lines are the corrected calculations, and the dashed are the calculations without corrections	16
Figure 7.3 : Total cross section for the N-pair production in Au-Au collisions verses γ with two photon Monte Carlo model. Solid lines are the corrected calculations, and the dashed are the calculations without corrections	17
Figure 7.4 : Probability of producing N-pairs in a Au-Au as a function of impact parameter b with $\gamma = 100$ in two photon Monte Carlo model for $a = 1.8\lambda_c$. Solid lines are the corrected calculations, and the dashed are the calculations without corrections	18
Figure 7.5 : Differential cross section for the N-pair production in Au-Au collision with $\gamma = 100$ in two photon Monte Carlo model for $a = 1.8\lambda_c$. Solid lines are the corrected calculations, and the dashed are the calculations without corrections	18
Figure 7.6 : Total cross section for the N-pair production in Au-Au collisions verses γ with two photon Monte Carlo model for $a = 1.8\lambda_c$. Solid lines are the corrected calculations, and the dashed are the calculations without corrections	19
Figure 8.1 : Probability of producing N-pairs in a Pb-Pb collision as a function of impact parameter b with $\gamma = 3400$ in two photon monte carlo model. Solid lines are the corrected calculations, and the dashed are the calculations without corrections	21

Figure 8.2 :	Differential cross section for the N-pair production in Pb-Pb collision with $\gamma = 3400$ in two photon monte carlo model. Solid lines are the corrected calculations, and the dashed are the calculations without corrections	22
Figure 8.3 :	Total cross section for the N-pair production in Pb-Pb collisions verses γ in two photon monte carlo model. Solid lines are the corrected calculations, and the dashed are the calculations without corrections	22
Figure 8.4 :	Probability of producing N-pairs in a Pb-Pb collision as a function of impact parameter b with $\gamma = 3400$ in two photon Monte Carlo model for $a = 4.7\lambda_c$. Solid lines are the corrected calculations, and the dashed are the calculations without corrections	23
Figure 8.5 :	Differential cross section for the N-pair production in Pb-Pb collision with $\gamma = 3400$ in two photon Monte Carlo model for a=4.7. Solid lines are the corrected calculations, and the dashed are the calculations without corrections	24
Figure 8.6 :	Total cross section for the N-pair production in Pb-Pb collisions verses γ in two photon Monte Carlo model for a=4.7. Solid lines are the corrected calculations, and the dashed are the calculations without corrections	24

LIST OF SYMBOLES

γ	: Lorentz factor
Z	: Charge
b	: Impact parameter
σ^c	: Coulomb correction cross section
α	: Structure parameter
λ_c	: Compton wavelenght
N	: Number of produced pairs
T	: Time ordering operator
β	: Velocity

LEPTON-PAIR PRODUCTION IN RELATIVISTIC HEAVY ION COLLISIONS : COULOMB CORRECTIONS TO TWO PHOTON MONTE CARLO MODEL

SUMMARY

The primary goal of modern particle accelerators is to get information about QGP which is thought to be the state of matter in the early seconds of universe. After Big Bang, at the temperature of $10^{12}K$, quarks and gluons, which are the constituents of baryons and mesons, are thought to be deconfined in the QGP. In particle accelerators heavy-ions are accelerated to collide and attain the thermodynamic conditions in which QGP is formed. However the thermodynamic conditions attained by any collision in particle accelerators may not be sufficient to form QGP. Two different collisions of heavy-ions occur in particle accelerators. To form QGP the heavy ions collide head-on. However the probability of a head-on collision to occur is low. Most ions in the beam collide peripherally. In peripheral collisions, interactions with high energies lead to lepton pair productions. Since QGP includes lepton pairs too, the cross sections are calculated to examine the production process and the physical properties of the produced particles. There are perturbative and nonperturbative approaches to calculate the associated cross sections of particles. We studied on a perturbative approach, which is called two photon Monte Carlo method, among many other perturbative approaches. The two photon model is based on a semi-classical model of the colliding ions and produced pairs. The cross sections are obtained with Feynman diagrams. Monte Carlo method is applied to obtain a solution for the cross sections. However these solutions do not include Coulomb fields of the heavy-ions in which the produced leptons scatter. Adding this contribution to the obtained cross sections is called Coulomb correction. To get a more precise result, we added Coulomb corrections to the cross sections obtained by two photon Monte Carlo method. We investigated the behavior of production probability, differential and total cross sections for the pairs produced in Au-Au and Pb-Pb collisions. The unexpected behavior of the functions for some particular range, revealed some problems of the two photon Monte Carlo method and showed that, the boundaries should be defined to use this method as a solution.

RÖLATİVİSTİK HIZLARDAKİ AĞIR İYON ÇARPIŞMALARINDA LEPTON ÇİFTİ ÜRETİMİ: İKİ FOTON MONTE CARLO YÖNTEMİNE COULOMB DÜZELTMELERİ

ÖZET

Günümüz parçacık hızlandırıcılarının birincil amacı, evrenin ilk saniyelerinde maddenin bulunduğu hal olan kuark gluon plazması hakkında bilgi edinmektir. Büyük patlamadan sonra 10^{12} Kelvin derece sıcaklıklarda baryon ve mezonların yapıtaşı olan kuark ve gluonların serbest halde bulunduğu düşünülmektedir. Kuark gluon plazmanın olduğu termodinamik koşulları sağlamak üzere ağır iyonlar, parçacık hızlandırıcılarda, ışık hızlarına yakın hızlarda çarpıştırılırlar. Ancak hızlandırıcılardaki herhangi bir çarpışmanın oluşturduğu koşullar kuark gluon plazmanın oluşması için yeterli olmayabilir. Hızlandırıcılarda iki tür çarpışma gerçekleşir. Kuark-gluon plazmanın oluşması için ağır iyonların, bu iki çarpışma türünden biri olan kafa kafaya çarpışmayı gerçekleştirmeleri gerekir. Ancak bu çarpışmaların gerçekleşme olasılıkları düşüktür. Demetteki iyonlardan çoğu sadece birbirlerine yaklaşarak geçerler. Bu durumda söz konusu olan yüksek enerjili etkileşimler ile lepton çiftleri yaratılır. Kuark gluon plazması da lepton çiftleri içerdiğinden, lepton çiftlerinin oluşum sürecini anlamak ve birbirinden ayırt etmek önemlidir. Bunun için oluşan lepton çiftlerinin tesir kesitleri hesaplanır. İlgili tesir kesitini hesaplama sürecinde pertürbatif ve pertürbatif olmayan yaklaşımlar izlenir. Biz de tesir kesitlerini hesaplamak için kullanılan bir çok pertürbatif yöntem arasında olan iki foton Monte Carlo yöntemi ile çalıştık. Bu yöntemde, ağır iki iyonun çarpışması ve lepton çifti üretilmesi yarı klasik olarak incelenir. İlgili tesir kesiti ifadeleri Feynmann diyagramları kullanılarak elde edilir. Bu ifadeler Monte Carlo tekniği kullanılarak hesaplanır. Ancak bu şekilde elde edilen tesir kesiti çözümleri yaratılan lepton çiftlerinin saçıldığı, çarpışan ağır iyonlara ait olan Coulomb alanlarını içermez. Bu etkinin elde edilmiş olan tesir kesitine eklenmesine Coulomb düzeltmesi denir. Daha doğru bir çözüme ulaşmak için, tesir kesitlerine Coulomb düzeltmelerini ekleyip Au-Au ve Pb-Pb iyonları çarpışmalarındaki parçacık oluşma olasılık fonksiyonlarının, diferansiyel ve toplam tesir kesitlerinin davranışlarını inceledik. Beklediğimiz davranışların belli durumlar için gözlenememesi, iki foton Monte Carlo tekniğinin bazı problemleri olduğunu ve çözüm olarak kullanılabilmesi için sınırlarının belirlenmiş olması gerektiğini ortaya çıkardı.

1. INTRODUCTION

The Relativistic Heavy Ion Collider (RHIC) at Brookhaven National Laboratory and Large Hadron Collider in Cern (LHC) investigate the quark-gluon plasma (QGP) which is believed to be form of matter in the early seconds of universe and may exist in the cores of neutron stars. To attain thermodynamic conditions in which quarks and gluons, constituents of baryons and mesons, become deconfined in QGP, heavy ions are accelerated to nearly speed of light to collide. However when the accelerated beams of ions meet, two different collisions occur; Head-on and peripheral collisions.

Formation of QGP may form in only one type of these collisions; When nuclei collide head-on [1]. The energy they have had transform to heat. The temperature may exceed 10^{12} degrees above absolute zero and phase transition happen. Protons and neutrons melt to liberate quarks and gluons and many other particles in such conditions. The leptons produced with the head-on collisions carry direct information about the early time universe [2,3].

When nuclei miss each other which is called peripheral collision, different physics is studied. This time the thermodynamic conditions attained are not sufficient to form QGP but intense enough to produce large number of electron-positron pairs, muon pairs, vector bosons and possibly the yet unconfirmed Higgs boson from the vacuum. [4–6] Since QGP contains leptons too, the electromagnetic production of these, from vacuum masks the signals of the pairs produced from hadronic interactions, fundamentally different from other production mechanism, and forms the major component of a physical background [7–9]. Pair production from the vacuum by electromagnetic interaction is therefore must be understood in detail and distinguished from other production mechanism.

The thermodynamic conditions associated with collisions are characterized by the Lorentz factor γ which is the kinetic energy per nucleon and the charges Z of the

ions in the beam. As the Lorentz factor increases more energetic beams leading to more momentum transfer are obtained.

For RHIC, $\gamma = 100$ for $Z=79$ Au collisions.

For LHC, $\gamma = 3400$ for $Z=82$ Pb collisions.

To examine the physical properties of the produced pairs cross sections are calculated.

2. SEMICLASSICAL APPROACH

In the semiclassical approach to peripheral collisions, the heavy ions are represented by time dependent classical fields in which the electron states evolve [10].

Nuclei approach each other through the axis perpendicular to the axis of the impact parameter, in the center of momentum frame.

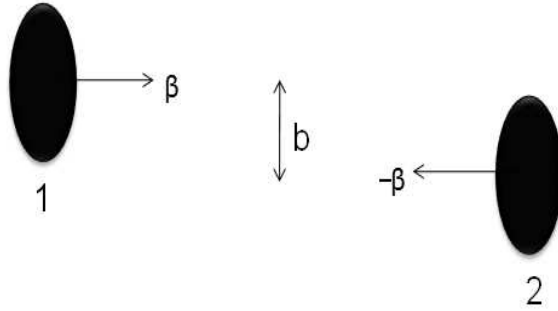


Figure 2.1: Schematic diagram of a relativistic heavy ion collision

The semiclassical coupling of the electrons to the electromagnetic field is given by the lagrangian [11];

$$L_{int} = -\bar{\psi}(x)\gamma_{\mu}\psi(x)\mathbf{A}^{\mu}(x) \quad (2.1)$$

where $A^{\mu}(x)$ is the total classical four-potential of the heavy ions 1 and 2.

In order to obtain the expression for the associated field, the four-potential in the rest frame of a point charge, Z , centered at the coordinates $(0, \frac{b}{2}, 0)$, is determined.

$$\mathbf{A}' = 0 \quad (2.2)$$

$$A'_0 = \frac{-Ze}{\sqrt{x'^2 + (y'^2 - \frac{b}{2})^2 + z'^2}} \quad (2.3)$$

In momentum space;

$$\begin{aligned}
A_0 &= \int dr_0 e^{iq'_0 \cdot r_0} \int d^3\mathbf{r} e^{-i\mathbf{q}' \cdot \mathbf{r}} A'_0(\mathbf{r}') \\
&= -2\pi Z e \delta(q'_0) e^{-iq_y \frac{b}{2}} \frac{4\pi}{q'^2}.
\end{aligned} \tag{2.4}$$

Lorentz transformation of the potential, to the frame moving with a relativistic velocity, $\boldsymbol{\beta}$, is made by transforming the momenta to this frame.

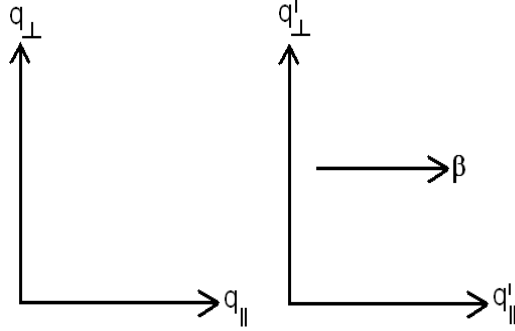


Figure 2.2: Coordinate frames

$$\begin{aligned}
q'_0 &= \gamma(q_0 + \boldsymbol{\beta} \mathbf{q}_{\parallel}) \\
\mathbf{q}'_{\parallel} &= \gamma(\mathbf{q}_{\parallel} + \boldsymbol{\beta} q_0) \\
\mathbf{q}'_{\perp} &= \mathbf{q}_{\perp}
\end{aligned} \tag{2.5}$$

Since \mathbf{A}'^{μ} transforms as a four-vector, we write;

$$\begin{aligned}
A_0(q_0) &= \gamma(A'_0 - \boldsymbol{\beta} \mathbf{A}'_{\parallel}) = \gamma A'_0 \\
\mathbf{A}_{\parallel}(\mathbf{q}_{\parallel}) &= \gamma(\mathbf{A}_{\parallel} - \beta A'_0) = -\gamma \boldsymbol{\beta} A'_0 \\
\mathbf{A}_{\perp}(\mathbf{q}) &= \mathbf{A}'_{\perp} = 0
\end{aligned} \tag{2.6}$$

Using 2.4 and 2.6,

$$\begin{aligned}
A^0(1) &= -8\pi^2 Z \gamma^2 \frac{\delta(q_0 - \boldsymbol{\beta} \mathbf{q}_{\mathbf{z}})}{q_z^2 + \gamma^2(q_x^2 + q_y^2)} e^{i\mathbf{q}_{\perp} \cdot \frac{b}{2}} \\
\mathbf{A}^z(1) &= \boldsymbol{\beta} A^0(1) \\
\mathbf{A}^{\mu}(1) &= A^0(1) + \mathbf{A}^z(1)
\end{aligned} \tag{2.7}$$

Since we work in the momentum frame, the velocity and the position of the nucleus 2 is obtained by the substitutions $\mathbf{b} \rightarrow -\mathbf{b}$ and $\boldsymbol{\beta} \rightarrow -\boldsymbol{\beta}$.

The electron states evolve in the sum of the associated fields calculated.

$$\mathbf{A}^\mu = \mathbf{A}^\mu(1) + \mathbf{A}^\mu(2) \quad (2.8)$$

Given the lagrangian 2.1, a semiclassical action is constructed in terms of a time dependent many electron state $\Phi(t)$.

$$\mathcal{S} = \int d^4x \langle \Phi(t) | L_0(x) + L_{int}(x) | \Phi(t) \rangle \quad (2.9)$$

where L_0 is the noninteracting fermion lagrangian given by 2.10

$$L_0 = \bar{\psi}(x)(\gamma_\mu i\partial^\mu - m)\psi(x) \quad (2.10)$$

The initial state vector is assumed to correspond to the vacuum state.

$$\lim_{t \rightarrow -\infty} |\Phi(t)\rangle \rightarrow |0\rangle = 1. \quad (2.11)$$

By this construction the Hamiltonian is well-defined and single particle states form a complete and orthonormal set as in 2.12

$$\sum_q |\chi_q^{(+)}\rangle \langle \chi_q^{(+)}| + |\chi_q^{(-)}\rangle \langle \chi_q^{(-)}| \quad (2.12)$$

Time evolution of the states is assumed to be governed by unitary dynamics; that is,

$$|\Phi(t)\rangle = K(t, -\infty)|0\rangle \quad (2.13)$$

where $KK^\dagger = K^\dagger K = 1$

Equations of motion are cast into the form;

$$i\partial_t K(t, t') = H(x)K(t, t') \quad (2.14)$$

where the interaction hamiltonian is constructed by the classical potentials of heavy ions.

$$H(t) = H_0(t) + V(t)$$

$$H_0(x) = -i\boldsymbol{\alpha} \cdot \boldsymbol{\nabla} + \gamma_0 m \quad (2.15)$$

$$V(x) = -\boldsymbol{\alpha} \cdot \mathbf{A}(x) + A_0(x)$$

The solutions obtained from the equations of motion are perturbative in \mathbf{A}^μ and expressed as the series;

$$K(t, \infty) = K_0(t, -\infty) + (-i) \int_{-\infty}^t d\tau K_0(t, \tau) V(\tau) K_0(\tau, -\infty) + \\ (-i)^2 \int_t^{-\infty} d\tau \int_{-\infty}^{\tau} d\tau' K_0(t, \tau) V(\tau) K_0(\tau, \tau') V(\tau') K_0(\tau', -\infty) + \dots \quad (2.16)$$

The total cross section is written in terms of the multiplicity of produced electrons, $\mathcal{N}_s(\mathbf{b})$, which represents the mean number of electrons produced out of vacuum.

$$\sigma = \int d^2b \mathcal{N}(\mathbf{b}) \quad (2.17)$$

Multiplicity is written as;

$$\mathcal{N} = \sum_{k>0} \langle 0 | S^\dagger a_k^\dagger a_k S | 0 \rangle = \sum_{k>0} \sum_{q<0} |\langle \chi_k^{(+)} | S | \chi_q^{(-)} \rangle|^2 \quad (2.18)$$

where 'a' is the annihilation operator and S is the associated scattering matrix given by 2.19

$$S = T[\exp(-i \int d^4x \mathcal{H}_{int}(x))] \quad (2.19)$$

The summation over the states k are restricted for particles and q for antiparticles. $|\chi^{(+)}\rangle$ represents single-particle states and $|\chi^{(-)}\rangle$ represents the single-antiparticle states.

Hence the differential cross section as a function of impact parameter is obtained as [11];

$$\frac{d\sigma}{db} = \sum_{k>0} \sum_{q<0} |\langle \chi_k^{(+)} | S | \chi_q^{(-)} \rangle|^2 \quad (2.20)$$

3. TWO PHOTON APPROACH

The two photon approach develops perturbative solutions to 2.14 and 2.20 to calculate the inclusive cross section obtained semiclassically, by using Feynmann theory. The contributions to scattering amplitude S , are from the two lowest order Feynmann diagrams [10]. These terms corresponds to second order terms in the perturbative solution of the propagator and represent the summation over possible time orderings, including the terms with crossed photon lines. [12]

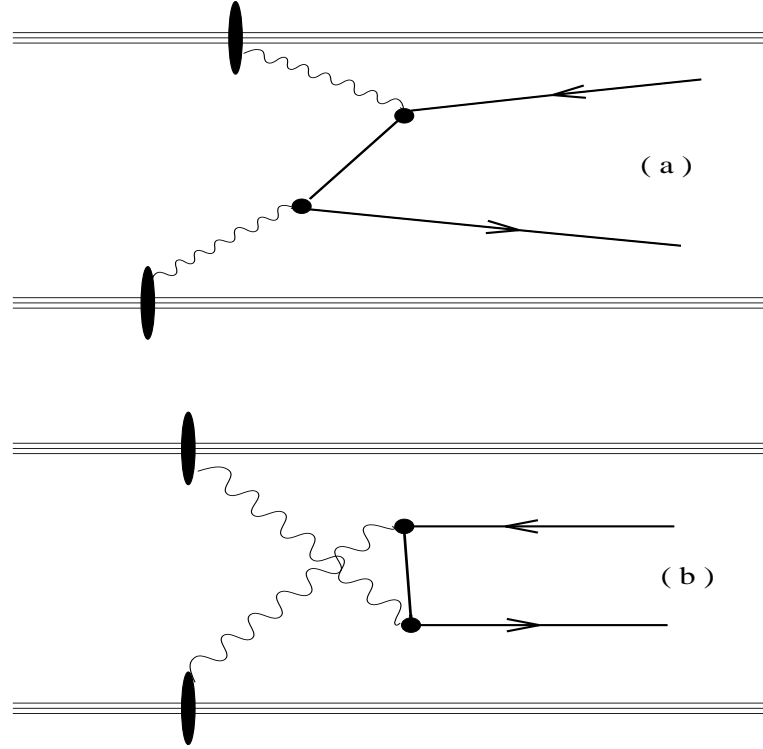


Figure 3.1: The direct(a) and indirect(b) Feynmann diagrams for pair production in a heavy ion-collision

Both the direct and indirect diagrams contribute to the total scattering matrix.

$$S = S_{12} + S_{21} \quad (3.1)$$

Using 3.1 for the differential cross section,

$$\frac{d\sigma}{db} = \sum_{k>0} \sum_{q<0} |\langle \chi_k^{(+)} | S | \chi_q^{(-)} \rangle|^2$$

$$\frac{d\sigma}{db} = \sum_{k>0} \sum_{q<0} |\langle \chi_k^{(+)} | S_{12} | \chi_q^{(-)} \rangle + \langle \chi_k^{(+)} | S_{21} | \chi_q^{(-)} \rangle|^2, \quad (3.2)$$

the differential cross section is calculated as [11];

$$\begin{aligned} \frac{d\sigma}{db} = \frac{1}{4\beta^2} \sum_{\sigma_k \sigma_q} \int \frac{d^3k}{(2\pi)^3} \frac{d^3q}{(2\pi)^3} \frac{d^2p_\perp}{(2\pi)^2} \frac{d^2p'_\perp}{(2\pi)^2} e^{i(\mathbf{p}_\perp - \mathbf{p}'_\perp) \cdot \mathbf{b}} \\ \times |A^{(+)}(k, q : \mathbf{p}_\perp) + A^{(-)}(k, q : \mathbf{k}_\perp + \mathbf{q}_\perp - \mathbf{p}_\perp)| \\ \times |A^{(+)}(k, q : \mathbf{p}'_\perp) + A^{(-)}(k, q : \mathbf{k}_\perp + \mathbf{q}_\perp - \mathbf{p}'_\perp)|^* \end{aligned} \quad (3.3)$$

and the total cross section is [11];

$$\sigma = \frac{1}{4\beta^2} \sum_{\sigma_k \sigma_q} \int \frac{d^3k}{(2\pi)^3} \frac{d^3q}{(2\pi)^3} \frac{d^2p_\perp}{(2\pi)^2} \times |A^{(+)}(k, q : \mathbf{p}_\perp) + A^{(-)}(k, q : \mathbf{k}_\perp + \mathbf{q}_\perp - \mathbf{p}_\perp)|^2 \quad (3.4)$$

where,

$$A^{(+)}(k, q : \mathbf{p}_\perp) = F(\mathbf{k}_\perp - \mathbf{p}_\perp : \omega_1) F(\mathbf{k}_\perp - \mathbf{p}_\perp : \omega_2) \mathcal{T}_{kq}(\mathbf{p}_\perp : +\beta) \quad (3.5)$$

$$A^{(-)}(k, q : \mathbf{p}_\perp) = F(\mathbf{k}_\perp - \mathbf{p}_\perp : \omega_2) F(\mathbf{k}_\perp - \mathbf{p}_\perp : \omega_1) \mathcal{T}_{kq}(\mathbf{p}_\perp : -\beta) \quad (3.6)$$

Function F corresponds to the scalar part of the field.

$$F(\mathbf{q} : \omega) = \frac{4\pi Z \gamma^2 \beta^2}{\omega^2 + \beta^2 |\mathbf{q}|^2} \quad (3.7)$$

For $F(\mathbf{k}_\perp - \mathbf{p}_\perp : \omega_1)$ and $F(\mathbf{k}_\perp - \mathbf{p}_\perp : \omega_2)$, ω_1 and ω_2 are the frequencies of the fields 1 and 2 of the heavy ions.

$$\omega_1 = \frac{E_q^{(-)} - E_k^{(+)} + \boldsymbol{\beta}(\mathbf{q}_\perp - \mathbf{k}_\perp)}{2} \quad (3.8)$$

$$\omega_2 = \frac{E_q^{(-)} - E_k^{(+)} - \boldsymbol{\beta}(\mathbf{q}_\perp - \mathbf{k}_\perp)}{2} \quad (3.9)$$

The amplitude \mathcal{T} relates the intermediate-photon lines to the out-going fermion lines. It explicitly depends on the velocity of the heavy ions, the transverse momentum and the states k, q .

$$\begin{aligned} \mathcal{T}_{kq}(\mathbf{p}_\perp : \boldsymbol{\beta}) = \sum_s \sum_{\sigma_p} [E_p^{(s)} - [\frac{E_k^{(+)} + E_q^{(-)}}{2}]] + \boldsymbol{\beta}[\frac{\mathbf{k}_\perp - \mathbf{q}_\perp}{2}]^{-1} \\ \times \langle u_{\sigma_k}^{(+)} | (1 - \boldsymbol{\beta} \boldsymbol{\alpha}_z) | u_{\sigma_p}^{(s)} \rangle \times \langle u_{\sigma_q}^{(s)} | (1 + \boldsymbol{\beta} \boldsymbol{\alpha}_z) | u_{\sigma_q}^{(-)} \rangle \end{aligned} \quad (3.10)$$

where $u_{\sigma}^{(s)}$ is the spinor parts of $\chi^{(s)}$

4. MONTE CARLO SOLUTION

The differential cross section 3.3 can be manipulated as [13];

$$\begin{aligned} \frac{d\sigma}{db} &= \frac{1}{4\beta^2} \sum_{\sigma_k \sigma_q} \int \frac{d^3\mathbf{k} \ d^3\mathbf{q} \ d^2\mathbf{p}_\perp \ d^2\mathbf{p}'_\perp}{(2\pi)^9} J_0(|\mathbf{p}_\perp - \mathbf{p}'_\perp| \cdot \mathbf{b}) \\ &\times |A^{(+)}(k, q : \mathbf{p}_\perp) + A^{(-)}(k, q : \mathbf{k}_\perp + \mathbf{q}_\perp - \mathbf{p}_\perp)| \\ &\times |A^{(+)}(k, q : \mathbf{p}'_\perp) + A^{(-)}(k, q : \mathbf{k}_\perp + \mathbf{q}_\perp - \mathbf{p}'_\perp)|^* \end{aligned} \quad (4.1)$$

$$\frac{d\sigma}{db} = \int_0^\infty d\mathbf{q} \ d\mathbf{b} \ J_0(\mathbf{q}\mathbf{b}) \ \mathcal{F}(\mathbf{q}) \quad (4.2)$$

where $J_0(\mathbf{q}\mathbf{b})$ is the Bessel function of order zero and $\mathcal{F}(\mathbf{q})$ is the nine-dimensional integral.

To solve equation 4.2 Monte Carlo technique is applied but since the Bessel function, $J_0(\mathbf{q}\mathbf{b})$, is a rapidly oscillating function, Monte Carlo technique is applied to solve only the nine-dimensional integral $\mathcal{F}(\mathbf{q})$ for fixed values of \mathbf{q} .

Numeric calculations indicate that $\mathcal{F}(\mathbf{q})$ has the form;

$$\mathcal{F}(\mathbf{q}) = \mathcal{F}(0)e^{-a\mathbf{q}} = \sigma_T e^{-a\mathbf{q}} = C_\infty \sigma_0 \ln^3(\gamma) e^{-a\mathbf{q}} \quad (4.3)$$

where $\mathcal{F}(0)$ is the value of the function at $\mathbf{q}=0$, $C_\infty = 2.19$ is the fitted parameter, $\sigma_0 = \lambda_c^2 Z_1^2 Z_2^2 \alpha^4$ is the reduced cross section and “a” is the slope of the graph shown below and computed as $1.35\lambda_c$.

Using 4.3 the differential cross section becomes;

$$\begin{aligned} \frac{d\sigma}{db} &= \int_0^\infty d\mathbf{q} \ d\mathbf{b} \ J_0(\mathbf{q}\mathbf{b}) \mathcal{F}(\mathbf{q}) \\ &= C_\infty \sigma_0 \ln^3(\gamma) \int_0^\infty d\mathbf{q} \ \mathbf{q}\mathbf{b} \ J_0(\mathbf{q}\mathbf{b}) e^{-a\mathbf{q}} \\ &= C_\infty \sigma_0 \ln^3(\gamma) \frac{a\mathbf{b}}{(a^2 + b^2)^{3/2}} \end{aligned} \quad (4.4)$$

The probability for producing a single pair is;

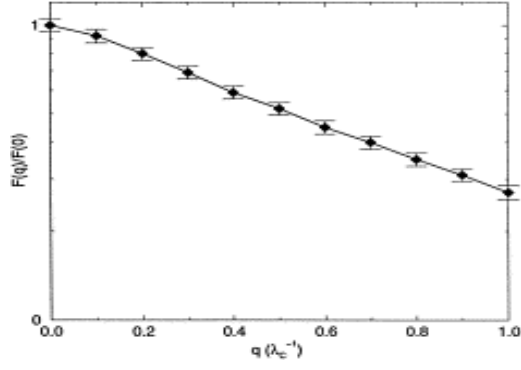


Figure 4.1: The function of $F(q)$ versus q for the charges of the heavy-ions between $Z_{1,2} = 20 - 90$ and for the energies between $\gamma = 10 - 3400$.

$$\mathcal{P}(b) = \frac{1}{2\pi\mathbf{b}} \frac{d\sigma}{db} \quad (4.5)$$

Using 4.4 in 4.5

$$\mathcal{P}(b) = \frac{1}{2\pi} C_{\infty} \lambda_c^2 Z_1^2 Z_2^2 \alpha^4 \ln^3(\gamma) \frac{a}{(a^2 + b^2)^{3/2}} \quad (4.6)$$

5. MULTI-PAIR PRODUCTION

For sufficiently high energies, the probability for producing more than one pair increases and contributes the total cross section . In addition, for high energy and large Z range, the perturbative probability for producing a single pair 4.6, obtained by two-photon approach violates unitarity [14]. To solve the unitarity problem and to obtain a probability which includes the number of produced particles, multi-pair production is examined.

In two-photon approach the probability for producing a single-pair were obtained by the two lowest order Feynmann diagrams. In order to obtain an expression for multi-pair production probability, higher order Feynmann diagrams are included. The included diagrams are selected under the assumptions of [15,16];

- 1.The interaction is only between the electromagnetic fields of colliding heavy ions.The interaction between the produced pairs are neglected.
- 2.The interaction between the produced pairs and the electromagnetic fields of the ions is neglected.
- 3.Fermion loops, which have exactly two vertices attached to each of the ions, are included.

Fig.5.2 is an example of the diagrams which are not included and 5.1 is an example of a diagram included.

With these assumptions, calculations lead to Poisson expression for probability of producing N-pairs [16].

$$P_N(b) = \frac{\mathcal{P}(b)^N \exp[-\mathcal{P}(b)]}{N!} \quad (5.1)$$

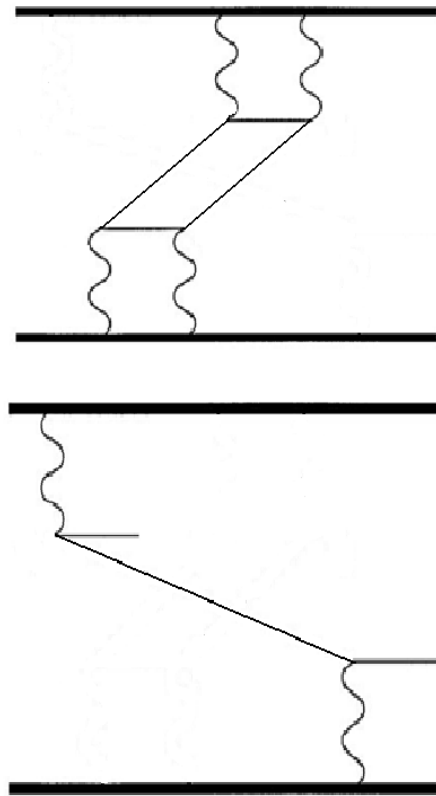


Figure 5.1: An example of a diagram included.

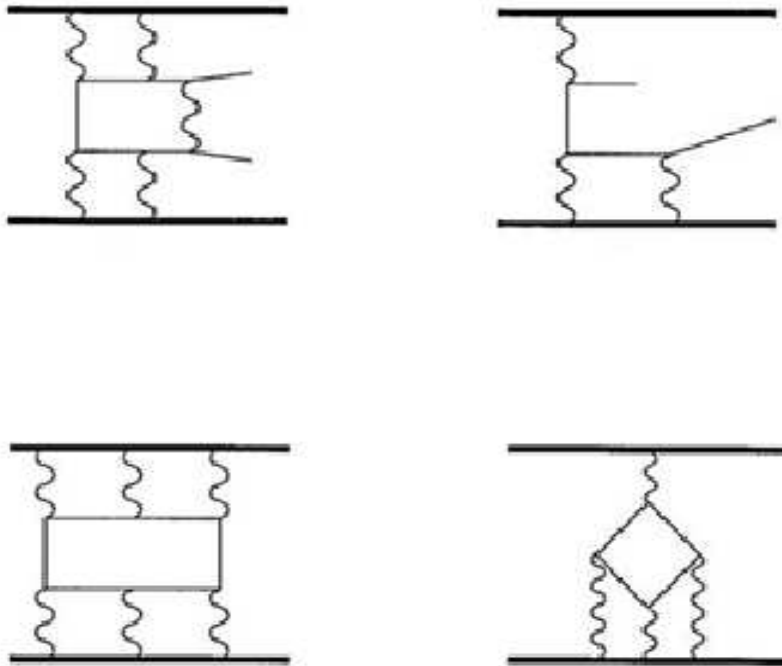


Figure 5.2: Diagrams which are not included.

6. COULOMB CORRECTIONS

To calculate the probability of multi-pair production, the electromagnetic interaction between the produced pairs and the fields of heavy ions were neglected. The cross section obtained by using the probability 5.1, is for the pairs scattered freely. Adding the contribution of the neglected interaction to the total cross section to obtain a precise expression, is called Coulomb corrections since the fields of the heavy ions are Coulomb fields [17].

The interaction between the produced pairs and the fields of ions is depicted in figure 6.1.

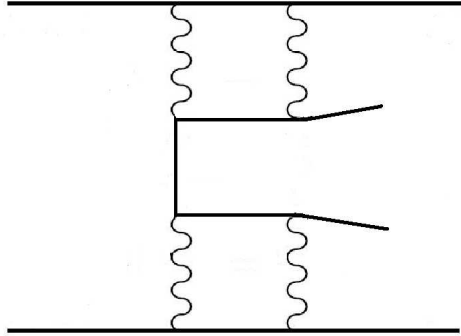


Figure 6.1: The interaction between the produced pairs and the fields of heavy ions.

Coulomb corrections are calculated, again semiclassically, as [18];

$$\sigma_1^c = -\frac{28(Z_1\alpha)^2(Z_2\alpha)^2}{9\pi m^2} f(Z_1\alpha) \ln^2(\gamma^2) \quad (6.1)$$

$$\sigma_2^c = -\frac{28(Z_1\alpha)^2(Z_2\alpha)^2}{9\pi m^2} f(Z_2\alpha) \ln^2(\gamma^2) \quad (6.2)$$

$$\sigma_{12}^c = \frac{56(Z_1\alpha)^2(Z_2\alpha)^2}{9\pi m^2} f(Z_1\alpha) f(Z_2\alpha) \ln^2(\gamma^2) \quad (6.3)$$

where

$$f(Z_{1,2}\alpha) = Z_{1,2}^2 \alpha^2 \sum_{n=1}^{\infty} \frac{1}{n(n^2 + Z_{1,2}^2 \alpha^2)} \quad (6.4)$$

7. CORRECTION IN Au-Au COLLISIONS

In RHIC, gold ions collide with $\gamma = 100$.

The probability for producing N-pair is given by 5.1. To obtain a more precise solution for a total cross section, we add Coulomb corrections to the production probability.

$$\begin{aligned}\mathcal{P}(b) &= \frac{1}{2\pi} C_{\infty} \lambda_c^2 Z_1^2 Z_2^2 \alpha^4 \ln^3(\gamma) \frac{a}{(a^2 + b^2)^{3/2}} \\ \mathcal{P}_{corr}(b) &= \left[\frac{1}{2\pi} C_{\infty} \lambda_c^2 Z_1^2 Z_2^2 \alpha^4 \ln^3(\gamma) + \sigma_1^c + \sigma_2^c + \sigma_{12}^c \right] \frac{a}{(a^2 + b^2)^{3/2}}\end{aligned}\tag{7.1}$$

where σ_1^c , σ_2^c and σ_{12}^c are given by 6.1, 6.2, 6.3 respectively.

In figure 7.1, we plotted the probabilities with and without corrections for the N-pair production in a Au-Au collision with $\gamma = 100$, in the collider frame. We see the effect of Coulomb corrections.

In the range where the impact parameter is lower than Compton wavelength of the electron, the probabilities for producing one and two-pairs are the same before adding Coulomb corrections. Adding the contribution of Coulomb corrections, decreases the probability for producing more than one-pair but increases the propability for producing one-pair. Such an increase in the cross section after adding a correction is unexpected.

In the range, where the impact parameter is greater than Compton wavelength of the electron, Coulomb correction additions decrease all the probabilities as expected.

In figure 7.2 we plotted the differential cross sections for N-pairs as a function of impact parameter. The effect of the corrections for the differential cross sections is the same as the production probabilities. In $b < \lambda_c$ range, Coulomb corrections increase the differential cross section for one-pair and decrease for more than

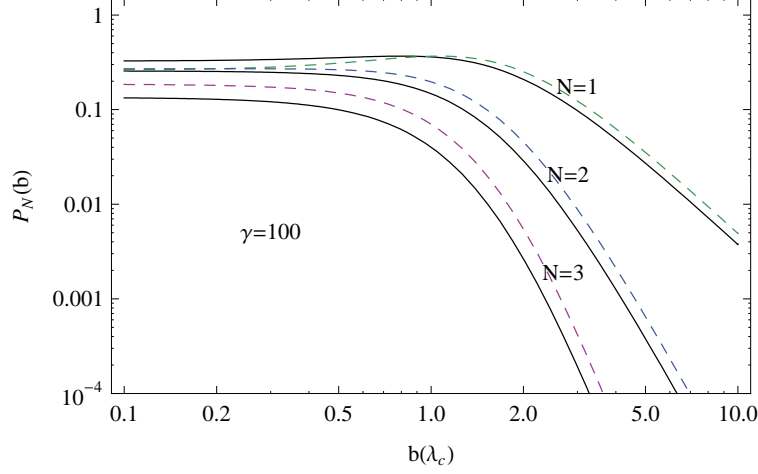


Figure 7.1: Probability of producing N -pairs in a Au-Au as a function of impact parameter b with $\gamma = 100$ in two photon Monte Carlo model. Solid lines are the corrected calculations, and the dashed are the calculations without corrections

one-pair. In $b > \lambda_c$ range, the cross sections for all pairs decrease with the addition of Coulomb corrections.

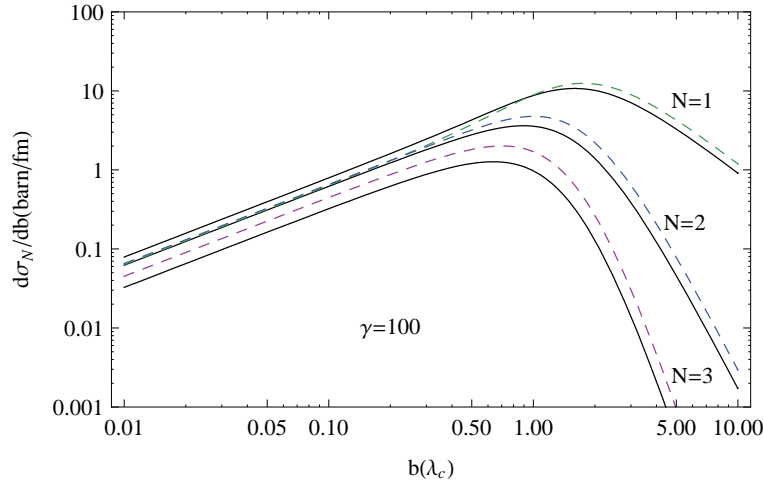


Figure 7.2: Differential cross section for the N -pair production in Au-Au collision with $\gamma = 100$ in two photon Monte Carlo model. Solid lines are the corrected calculations, and the dashed are the calculations without corrections

In figure 7.3 we plotted the total cross section as a function of γ . Coulomb corrections decrease the total cross sections for all pairs. For $b < \lambda_c$ range, the probability of producing one-pair and the total cross section for one-pair increased with Coulomb corrections. For total cross section, we do not encounter such a problem with one-pair. The graph is over all impact parameters, and the contributions of small impact parameters are negligible.

In table 7.2, we compared the total cross sections for Au-Au collisions.

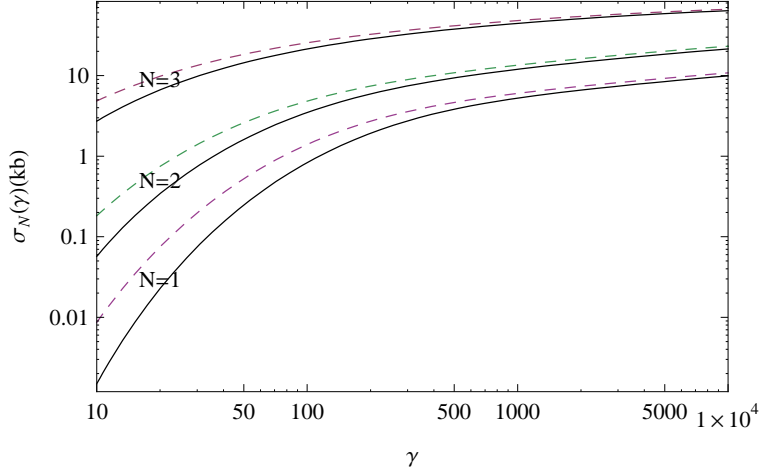


Figure 7.3: Total cross section for the N-pair production in Au-Au collisions verses γ with two photon Monte Carlo model. Solid lines are the corrected calculations, and the dashed are the calculations without corrections

Table 7.1: Total pair cross sections for Au-Au collisions.

$\gamma = 100$	$\sigma_{MC}(kb)$	$\sigma_{MC}^{corr.}(kb)$
N=1	25.5	21.4
N=2	4.8	3.5
N=3	1.4	0.8

The Coulomb corrections reduce the total cross sections; %16 for N=1, %28 for N=2, %40.5 for N=3.

Although the total cross sections decrease with Coulomb correction contribution, the increase in the production probability and the differential cross section of one-pair for small impact parameters, indicates a problem in the two photon Monte Carlo solution. We focused on the Monte Carlo part of the solution and saw that if the parameter “a”, which is the slope of the function $\mathcal{F}(\mathbf{q})$ given by 4.3, were greater, the production probability and the differential cross section for one-pair would not increase with Coulomb corrections.

We treated “a” as the cause of the problem and looked for a minimum value which satisfies the physical conditions we expect.

Originally “a” is $1.35\lambda_c$. We increased “a” until we reach the minimum value where the probability of producing one-pair with Coulomb corrections is higher than the same probability without corrections.

With $a = 1.8\lambda_c$, we reach the expected situation as in 7.4

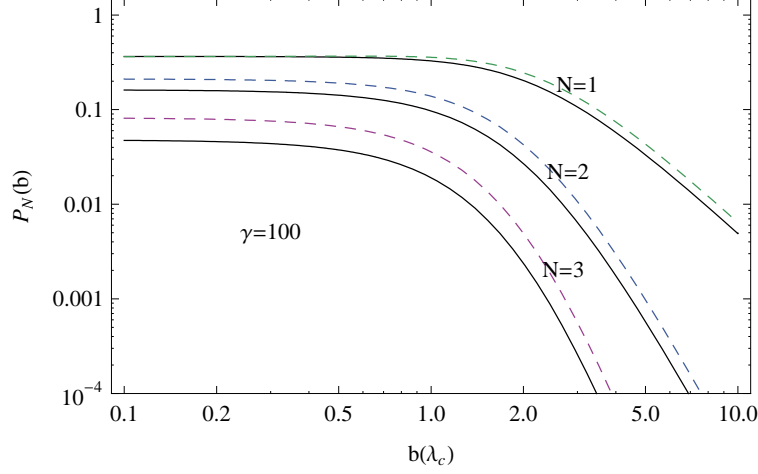


Figure 7.4: Probability of producing N -pairs in a Au-Au as a function of impact parameter b with $\gamma = 100$ in two photon Monte Carlo model for $a = 1.8\lambda_c$. Solid lines are the corrected calculations, and the dashed are the calculations without corrections

In 7.5 we plotted the differential cross section for $a = 1.8\lambda_c$. We also see that the behaviour of one and two-pairs are now different from each other, contrary to $a = 1.35\lambda_c$ case which also can be seen as a problem.

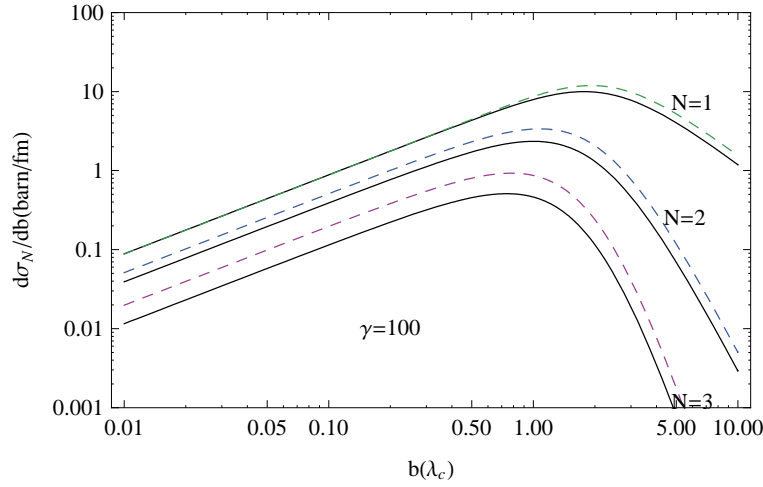


Figure 7.5: Differential cross section for the N -pair production in Au-Au collision with $\gamma = 100$ in two photon Monte Carlo model for $a = 1.8\lambda_c$. Solid lines are the corrected calculations, and the dashed are the calculations without corrections

In 7.6 we plotted the total cross section for $a = 1.8\lambda_c$.

Table 7.2: Total pair cross sections for Au-Au collisions with $a = 1.8\lambda_c$.

$\gamma = 100$	$\sigma_{MC}(kb)$	$\sigma_{MC}^{corr.}(kb)$
N=1	27.5	22.6
N=2	4	2.7
N=3	0.8	0.4

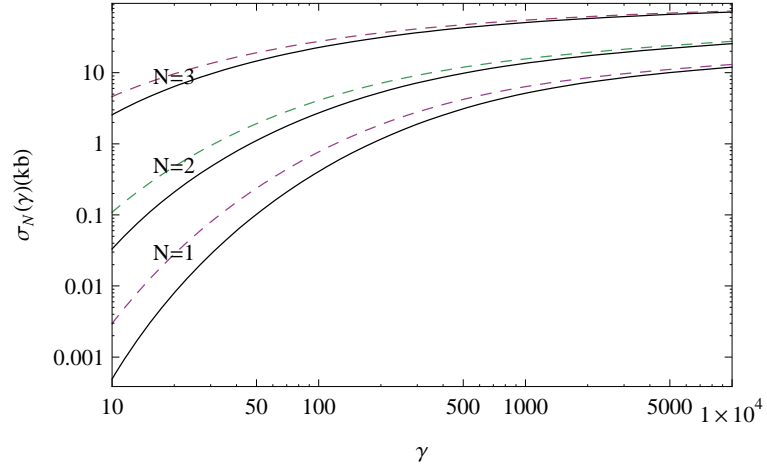


Figure 7.6: Total cross section for the N-pair production in Au-Au collisions versus γ with two photon Monte Carlo model for $a = 1.8\lambda_c$. Solid lines are the corrected calculations, and the dashed are the calculations without corrections

The Coulomb corrections reduce the total cross sections; %18 for N=1, %33 for N=2, %47 for N=3.

8. CORRECTION IN Pb-Pb COLLISIONS

In LHC, lead ions collide with $\gamma = 3400$

In figure 8.1 we plotted the probabilities with and without Coulomb corrections for the N-pair production in a Pb-Pb collision with $\gamma = 3400$, in the collider frame. We see the effect of Coulomb corrections.

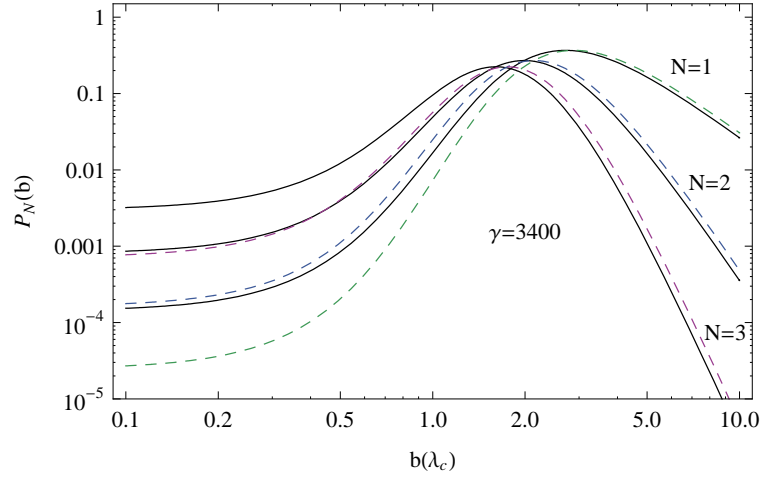


Figure 8.1: Probability of producing N-pairs in a Pb-Pb collision as a function of impact parameter b with $\gamma = 3400$ in two photon monte carlo model. Solid lines are the corrected calculations, and the dashed are the calculations without corrections

For small impact parameters in Pb-Pb collisions, the probabilities for producing N-pairs increase with the impact parameter and we see the problem without the aid of Coulomb corrections. An increase in the production probability with the increasing impact parameter, does not seem physical. In this case, we cannot limit the nonphysical situation with an impact parameter lower than Compton wavelength. The probabilities continue increasing for the impact parameters greater than Compton wavelength. In this range, where the probabilities increase with impact parameter, Coulomb corrections also increase the same probabilities. However the probabilities start decreasing after reaching a maximum value and Coulomb corrections reduce the probability. For this range the results are physical.

In figure 8.2 we plotted the differential cross sections of N-pairs as a function of impact parameter. The effect of the corrections for the differential cross sections is the same as the production probabilities.

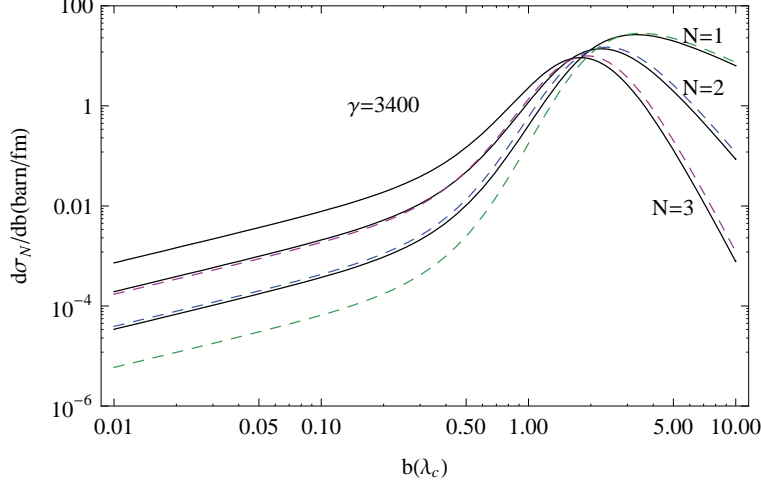


Figure 8.2: Differential cross section for the N-pair production in Pb-Pb collision with $\gamma = 3400$ in two photon monte carlo model. Solid lines are the corrected calculations, and the dashed are the calculations without corrections

The acceptable situation is only for the impact parameters which are greater than the impact parameter for the maximum differential cross section. In this range, the production probabilities decrease with the increasing impact parameter and Coulomb corrections reduce the differential cross sections as expected.

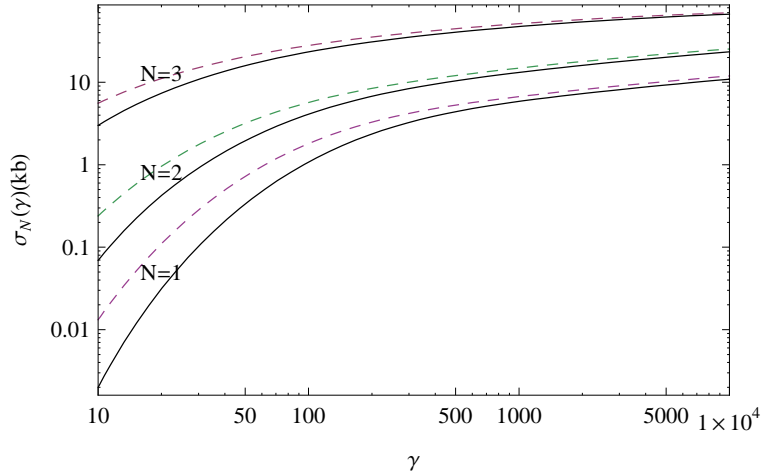


Figure 8.3: Total cross section for the N-pair production in Pb-Pb collisions verses γ in two photon monte carlo model. Solid lines are the corrected calculations, and the dashed are the calculations without corrections

In figure 8.3 we plotted the total cross section as a function of γ . Coulomb corrections decrease the total cross sections for all pairs as in Au-Au collisions since the total cross section is over all impact parameters.

In table 8.2, we compared the total cross sections for Pb-Pb collisions.

Table 8.1: Total pair cross sections for Pb-Pb collisions.

$\gamma = 3400$	$\sigma_{MC}(kb)$	$\sigma_{MC}^{corr.}(kb)$
N=1	62	58.7
N=2	20.2	18.4
N=3	9.3	8.4

The Coulomb corrections reduce the total cross sections; %5.5 for N=1, %9.3 for N=2, %10 for N=3.

The effect of Coulomb corrections for Pb-Pb collisions is less than as it is for Au-Au collisions. The problems we encountered in the region where the production probabilities increase with impact parameter and rise with Coulomb corrections may cause this effect.

To understand the problem, we applied the same procedure as in Au-Au collisions. We changed the constant “a” in the equation 4.3. We increased the value of “a” until we reach a minimum value which satisfies the physical conditions we expect.

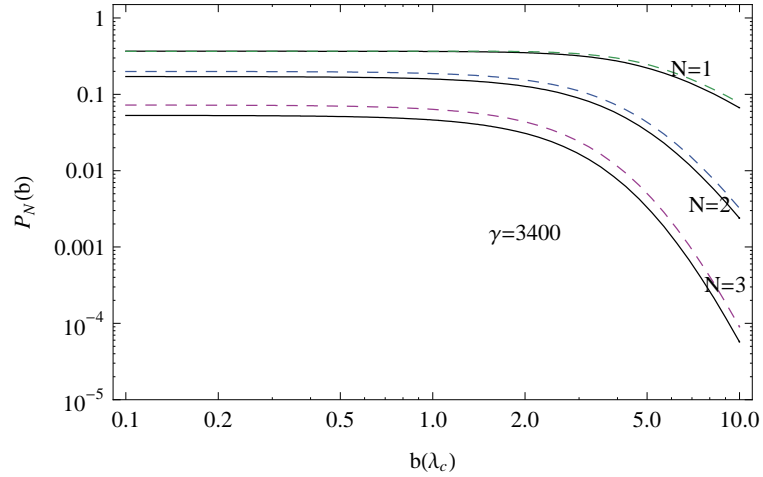


Figure 8.4: Probability of producing N-pairs in a Pb-Pb collision as a function of impact parameter b with $\gamma = 3400$ in two photon Monte Carlo model for $a = 4.7\lambda_c$. Solid lines are the corrected calculations, and the dashed are the calculations without corrections

In figure 8.4 we plotted the probability for producing N-pairs as a function of impact parameter for $a = 4.7\lambda_c$.

The differential cross section as a function of impact parameter and the total cross section as a function of γ is shown in figure 8.5 and 8.6 respectively.

For $a = 4.7\lambda_c$ we compared the total cross sections.

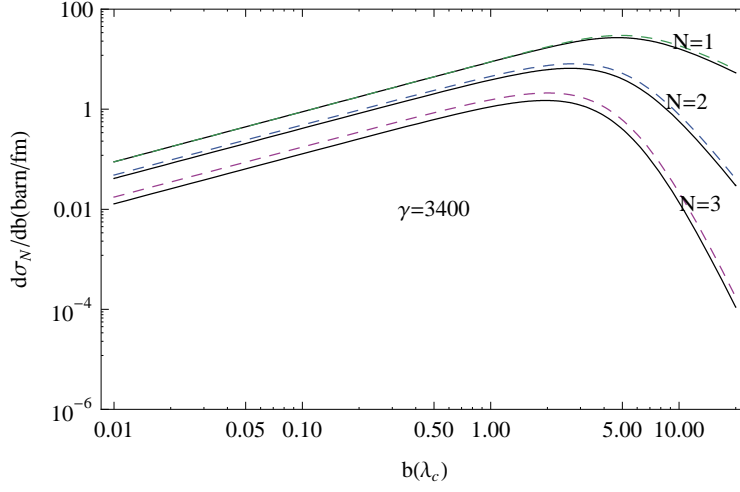


Figure 8.5: Differential cross section for the N-pair production in Pb-Pb collision with $\gamma = 3400$ in two photon Monte Carlo model for $a=4.7$. Solid lines are the corrected calculations, and the dashed are the calculations without corrections

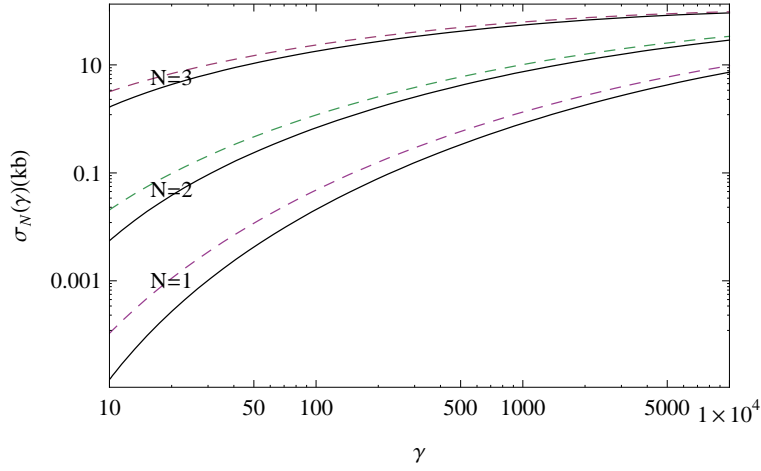


Figure 8.6: Total cross section for the N-pair production in Pb-Pb collisions verses γ in two photon Monte Carlo model for $a=4.7$. Solid lines are the corrected calculations, and the dashed are the calculations without corrections

Table 8.2: Total pair cross sections for Pb-Pb collisions with $a = 4.7\lambda_c$.

$\gamma = 3400$	$\sigma_{MC}(kb)$	$\sigma_{MC}^{corr.}(kb)$
N=1	83.4	76.8
N=2	21	17
N=3	4.4	3

Coulomb corrections reduce the total cross sections; %8 for $N=1$, %20 for $N=2$, %30.5 for $N=3$.

9. CONCLUSION

We added Coulomb corrections to the cross sections of lepton pairs produced by a peripheral heavy-ion collision. The cross sections of the produced pairs are obtained by two photon Monte Carlo approach. However adding Coulomb corrections reveals some problems of this model. For small impact parameters the corrections rises the resulting cross sections. For high energies the problem is greater. In a Pb-Pb collisions with $\gamma = 3400$, the production probability increases with impact parameter and Coulomb corrections. However after a limit of impact parameter which related with the γ factor of the collision, the results are completely acceptable. The production probability decreases with impact parameter and Coulomb corrections. These results show that, the two photon Monte Carlo approach is adequate to explain the physics of pair production only for a particular range. To obtain reliable solutions with the two photon Monte Carlo approach, the impact parameters which gives nonphysical results, should be isolated.

To understand the problem with the small impact parameters, we focused on the Monte Carlo solution of the two photon approach. We saw that, as the parameter “a” increases, the production probabilities for the small impact parameters get more reasonable. We used $a = 1.8\lambda_c$ for Au-Au collisions with $\gamma = 100$ and $a = 4.7\lambda_c$ for Pb-Pb collisions with $\gamma = 3400$. So we conclude that the value of “a” may not be constant and may depend on the γ factor or other parameters.

Our next step is to work on this problem. We are going to go over the Monte Carlo solution, examine the parameter “a” and try to understand whether it is the cause of the problem as we suspect.

REFERENCES

- [1] **Blaizot, J.P.**, 1991. Special issue on quark matter, *Nucl. Phys.A*, **525**, 64–111.
- [2] **Kajantie, K., Kataja, J., McLerran, L. and Russkanen, P.V.**, 1986. Studies of the hydrodynamic evolution of matter produced in fluctuations in p-p collisions and in ultrarelativistic nuclear collisions. II. Transverse momentum distributions, *Phys.Rev.D*, **34**, 2755.
- [3] **Kajantie, K., Kataja, J., McLerran, L. and Mekjian, A.**, 1986. Dilepton emission and the QCD phase transition in ultrarelativistic nuclear collisions, *Phys.Rev.D*, **34**, 2746.
- [4] **Bottcher, C. and Strayer, M.R.**, 1988. Relativistic Theory of Fermions and Classical Fields on a Collocation Lattice, *Nucl. Instrum. Methods B*, **31**, 122.
- [5] **Bottcher, C. and Strayer, M.R.**, 1989. Electron pair production from pulsed electromagnetic fields in relativistic heavy-ion collisions, *Phys.Rev.D*, **39**, 1330.
- [6] **Bottcher, C. and Strayer, M.R.**, 1990. Coherent electromagnetic production of mu an tau lepton pairs in relativistic heavy-ion collisions, *J.Phys.G*, **16**, 975.
- [7] **Kelly, H.P. and Kim, Y.**, 1985. Atomic theory workshop on relativistic and QED effects in heavy atoms, *AIP Conf.*, **136**.
- [8] **Bottcher, C. and Strayer, M.R.**, 1986. Physics of strong fields ,proceedings of the international advanced course, *NATO advanced study institute*, **153**, 629.
- [9] **Teller, E.**, 1986. Proceedings of the ninth international conference on the application of accelerators in research and industry, *NATO advanced study institute*.
- [10] **Bottcher, C. and Strayer, M.R.**, 1987. Relativistic Theory of Fermions and Classical Fields on a Collocation Lattice, *Annals of Physics*, **175**, 64–111.
- [11] **Bottcher, C. and Strayer, M.R.**, 1989. Electron pair production from pulsed electromagnetic fields in relativistic heavy-ion collisions, *Physical Review D*, **39**, 1330–1335.

- [12] **Block, F. and Nordsieck, A.**, 1937. Radiation Field of the electron, *Physical Review*, **52**, 54–59.
- [13] **Güçlü, M.C.** Semi-analytic calculations for the impact parameter dependence of electromagnetic multi-lepton pair production.
- [14] **Baur, G.**, 1990. Unitarity and electron pair production in peripheral ultra relativistic heavy-ion collisions, *Physical Review D*, **41**, 3535.
- [15] **Güçlü, M.C., Wells, J.C., Umar, A.S., Strayer, M.R. and Ernst, D.J.**, 1995. Impact-parameter dependence of multiple lepton-pair production from electromagnetic fields, *Physical Review A*, **51**, 1836–1844.
- [16] **Güçlü, M.C., Li, J., Umar, A.S., Ernst, D.J. and Stayer, M.R.**, 1999. Electromagnetic lepton-pair production in relativistic heavy-ion collisions, *Annals of physics*, **272**, 7–48.
- [17] **Güçlü, M.C., Yılmaz, M. and Kovankaya, G.**, 2005. Coulomb corrections in the lepton-pair production in ultra-relativistic nuclear collisions, *Phys. Rev. A*, **72**, 022724.
- [18] **Lee, R.N. and Milstein, A.I.**, 2001. Coulomb corrections and multiple electron-positron pair production in ultra-relativistic nuclear collisions, *Phys. Rev.A*, **64**, 032106.

CIRRICULUM VITA

Candidate's full name: Fatma Pınar ASLAN

Place and date of birth: Adana, 18th of January, 1982

Permanent Address: 34055, 34/9

Universities and Colleges attended:

2000-2005 Pyhsics Engineering - Bachelor of Science - Hacettepe University ,
ANKARA

2006-2009 Pyhsics Engineering - Master of Science - İstanbul Technical University
, İSTANBUL